https://ntrs.nasa.gov/search.jsp?R=19930087932 2020-06-17T11:45:33+00:00Z

RM E53I25

NACA RM E53I25

NACA

RESEARCH MEMORANDUM

ALTITUDE PERFORMANCE CHARACTERISTICS OF THE J73-GE-1A TURBOJET ENGINE

By Carl E. Campbell and E. William Conrad

Lewis Flight Propulsion Laboratory
Cleveland, Ohio

NATIONAL ADVISORY COMMITTEE FOR AERONAUTICS

WASHINGTON
December 9, 1954
Declassified August 19, 1960

NATIONAL ADVISORY COMMITTEE FOR AERONAUTICS

RESEARCH MEMORANDUM

ALTITUDE PERFORMANCE CHARACTERISTICS OF THE J73-GE-1A TURBOJET ENGINE

By Carl E. Campbell and E. William Conrad

SUMMARY

An investigation was conducted in an altitude test chamber at the NACA Lewis laboratory to determine the performance characteristics of the J73-GE-1A turbojet engine. This model engine had a fixed-area exhaust nozzle and was the first of a series of J73 production engines. Performance data were obtained at simulated altitudes from 15,000 to 55,000 feet and at flight Mach numbers from approximately 0.07 to 1.01, which correspond to a range of compressor-inlet Reynolds number index values from 0.90 to 0.13.

Engine performance is presented in the form of engine pumping characteristics and combustion efficiency, from which the over-all performance may be calculated for any flight condition within the range of Reynolds number indices covered by the experimental data. Curves of net thrust and fuel flow, computed from these data, are presented as functions of true airspeed for four altitudes. Data are also included to enable the determination of thrust in flight.

INTRODUCTION

An investigation was conducted in an altitude test chamber at the NACA Lewis laboratory to determine the complete performance and operational characteristics of the J73 turbojet engine. The first phase of this program, which is reported herein, was an altitude-performance evaluation of the J73-GE-1A engine. Pending development of an improved control, this engine had a turbine-nozzle area ten percent larger than the design area for later engine models in order to avoid compressor surge during flight tests. The engine also incorporated variable compressor-inlet guide vanes to avoid part-speed surge. Throughout the investigation reported herein, however, the guide vanes were fixed at the design angle for the high engine speed range (13° from axial).

The over-all altitude-performance characteristics of this engine are reported herein, and the component performance characteristics are given in reference 1. Data were obtained over a corrected engine speed range from 83 to 108 percent of rated speed, at altitudes from 15,000 to 55,000 feet, and at flight Mach numbers from approximately 0.07 to 1.01. The corresponding range of compressor-inlet Reynolds number index values was from 0.90 to 0.13.

The data are presented in the form of engine pumping characteristics to allow accurate calculation of engine performance at any operating or flight condition within the range covered by the experimental data. From the pumping characteristics, net thrust and fuel flow were calculated and are presented as functions of true airspeed for sea level and for altitudes of 15,000, 35,000, and 50,000 feet. A curve is also presented that will allow determination of thrust in flight by the measurement of ambient static pressure and total pressure in the exhaust nozzle.

INSTALLATION AND INSTRUMENTATION

Engine. - The J73-GE-1A turbojet engine (fig. 1) has variable compressor-inlet guide vanes, a 12-stage axial-flow compressor, ten cannular-type combustors, a two-stage turbine, and a fixed conical exhaust nozzle. At engine speeds above 6400 rpm, the variable inlet guide vanes are scheduled to be in the open position, with the tangent line between the leading and trailing edges at the blade tip forming an angle of 13° with the engine center line. At lower engine speeds, the guide vanes are scheduled to be in the closed position to avoid compressor surge, with the tangent line forming an angle of 43° with the engine center line. In addition to the inlet guide-vane variation, the turbine-nozzle area of the engine was increased to 110 percent of the design value for later engine models as a further precaution to avoid compressor surge until the engine control is refined. Compressor-outlet leakage and a small amount of bleed air are used for a balance-piston force at the front of the compressor and for cooling the turbine disks and the first-stage turbine nozzles. The exhaust nozzle (20.95-inch cold diameter) was sized to give the rated exhaust gas temperature of 1215° F at sea-level static conditions on a standard day at the rated engine speed of 7950 rpm. At these conditions, the rated engine thrust is 8630 pounds and the air flow is 142 pounds per second.

Altitude chamber. - The altitude chamber in which the engine was installed is shown schematically in figure 2. The test-chamber diameter is 14 feet. Atmospheric air or heated or refrigerated dry air can be supplied to the inlet of the test chamber. The engine was mounted on a movable test-bed, which was connected through linkages to a thrust-measuring cell of the null-type pressure-balanced diaphragm design. The thrust apparatus was calibrated by the dead-weight method with the engine and all connections in place.

The inlet or ram-pressure section of the chamber was separated from the exhaust or altitude-pressure section of the chamber by a bulkhead. A labyrinth-type frictionless seal was provided between the bulkhead and the engine-inlet duct to allow a slight amount of axial movement of the engine without binding. The bellmouth cowl was attached to the bulkhead and therefore transmitted no force to the engine-inlet duct.

Instrumentation. - The stations throughout the engine at which instrumentation was installed are shown in figure 3. Schematic drawings of the location of instrumentation at those stations that are pertinent in the determination of over-all engine performance are given in figure 4. All pressures were photographically recorded with either mercury- or alkazene-filled manometers. Temperatures were recorded by automatic self-balancing potentiometers. Engine speed was determined by a chronometric tachometer, and fuel flow was measured by means of calibrated rotameters.

PROCEDURE

Performance data were obtained at simulated altitudes from 15,000 to 55,000 feet and flight Mach numbers from 0.07 to 1.01. Engine speed was varied from approximately 6400 rpm to the rated speed of 7950 rpm. Lower engine speeds, at which the inlet guide vanes are scheduled to be in the closed position, were not obtained because of special instrumentation, which prevented movement of the guide vanes. During this phase of the investigation, full control of inlet-air temperatures was not possible; however, temperatures were obtained in the range from -25° to 40° F.

Fuel conforming to specification MIL-F-5624A grade JP-4 with a lower heating value of 18,700 Btu per pound and a hydrogen-carbon ratio of 0.168 was used throughout the investigation. Air flow was obtained from a survey of total and static pressures in the engine inlet at station 1 (fig. 3).

All symbols used in this report are defined in appendix A.

RESULTS AND DISCUSSION

All the over-all performance data obtained in the investigation of the engine are compiled in table I in both nongeneralized and generalized form. It should be noted that the data in nongeneralized form are not adjusted for slight differences between the actual and the NACA standard values of inlet pressure, exhaust pressure, or engine-inlet temperature.

Pumping characteristics. - If the exhaust-nozzle pressure ratio of a turbojet engine is sufficiently high that the flow coefficient is constant with increasing nozzle pressure ratio, the engine pressure ratio at any constant temperature ratio is a function only of corrected engine speed, exhaust-nozzle area, and Reynolds number. Except for the effect of Reynolds number, changes in altitude or flight Mach number have no effect on the engine pressure ratio at constant values of engine temperature ratio. Accordingly for the engine discussed herein, the pumping characteristics are completely defined by curves of engine pressure ratio against engine temperature ratio for several constant values of Reynolds number index. These curves, coupled with associated curves that give the air flow and combustion efficiency at various operating conditions, completely define the performance of the engine.

The engine speeds and flight Mach numbers above which the exhaust nozzle was choked are defined in figure 5. The solid curve denotes the conditions at which the average exhaust-nozzle pressure ratio corresponded to the critical value. However, the exhaust-nozzle flow coefficient had not reached its maximum value at the critical pressure ratio and continued to increase up to an exhaust-nozzle pressure ratio of about 2.2. The dashed line denotes the conditions at which the exhaust nozzle was considered completely choked; that is, the pressure ratio was above critical and the flow coefficient had reached its maximum value. The pumping characteristics of figure 6, however, may be used with only small error in the region between the two curves, but they are not valid at nozzle pressure ratios below choking or for different exhaust-nozzle areas. The curves of figure 5 were determined from cross plots of exhaust-nozzle pressure ratio against corrected engine speed. The solid curve required some extrapolation inasmuch as only a few data points were in the region where the average exhaust-nozzle pressure ratio was below the critical value. The data were sufficient, however, to show that there was no appreciable Reynolds number effect on the solid curve.

The pumping characteristics for this engine (fig. 6) are given in the form of curves of engine pressure ratio as a function of engine temperature ratio for a wide range of Reynolds number indices. The altitudes and flight Mach numbers simulated in obtaining the different values of Reynolds number index are included in the symbol key. Lines of constant corrected engine speed, in percent of rated speed, have been superimposed; and a comparison with the curves of figure 5 shows that the exhaust nozzle was choked for virtually all the data of figure 6. Examination of the data reveals that it was immaterial what combination of altitude and flight Mach number was used to obtain a given value of Reynolds number index for the range of engine speeds presented. Although the data obtained at Reynolds number indices of 0.54 and 0.39 fall slightly out of order, examination of the bulk of the data shows that, at constant corrected engine speed, a progressive increase in T_7/T_1 and decrease in P_7/P_1 occurred as the Reynolds number index was reduced. These changes result from reduced compressor efficiency and corrected air flow, as shown in reference 1.

Air flow. - The effect of Reynolds number index on engine air flow is shown in figure 7. Because of the data scatter, curves could not be drawn for Reynolds number index values of 0.16, 0.14, and 0.13. It is apparent, however, that the corrected air flow was reduced at a given corrected engine speed as the value of Reynolds number index was reduced.

Fuel flow. - Because of Reynolds number effects on component efficiencies and also because of variations in combustion efficiency with flight condition, the corrected fuel flow does not generalize to a single curve as a function of corrected engine speed. In order to permit the accurate determination of fuel flow, the combustion efficiency has been generalized as a function of the combustion parameter W_aT_7 (fig. 8). This parameter is shown to be proportional to the familiar parameter PT/V in reference 2. Both the air flow W_a and the exhaust-gas temperature T_7 can be obtained from figures 6 and 7, and the combustion efficiency can thus be determined. The ideal fuel-air ratio required to produce a given temperature rise from the engine inlet to the exhaust-nozzle inlet is given in figure 9 (data from ref. 3). The actual fuel-air ratio may be determined by dividing the ideal fuel-air ratio by the combustion efficiency. Fuel flow can then be obtained by multiplying the actual fuel-air ratio by the air flow.

Thrust. - By using the curves of figures 6 to 10 in conjunction with equation (5) of appendix B, jet thrust may be calculated on the basis of rake measurements at the exhaust-nozzle inlet at any value of Reynolds number index within the range covered. All values of rake jet thrust should be adjusted to actual thrust values by applying a thrust coefficient, that is, a calibration factor correlating rake thrust data with actual thrust data as determined from force measurements on the test-bed. However, inasmuch as the thrust coefficient was determined to be approximately 1.00 in this investigation, no adjustment was necessary. Net thrust can then be obtained from jet thrust by subtracting the momentum force of the inlet air. Also, the thrust may be calculated for various values of ram-pressure recovery or tail-pipe pressure loss by proper adjustment of the engine-inlet or exhaust pressures. A sample calculation is given in appendix C to illustrate the use of the curves.

Performance from pumping characteristics. - Net thrust and fuel flow for operation at standard NACA altitude conditions and 100-percent ram-pressure recovery have been calculated from the pumping characteristics and are shown as functions of true airspeed (fig. 10) for engine speeds of 100,.95, 90, and 85 percent of rated engine speed. The portion of the curves denoted by the broken line required extrapolation of the pumping-characteristic curves and may therefore be less accurate than the solid curves. The dot-dash curve of figure 10 defines the condition of limiting exhaust-gas temperature. It is seen from figure 10(a) that the exhaust nozzle used was very slightly smaller than required for limiting temperature at rated engine speed; limiting temperature occurred at about 99 percent of rated speed. From figures 10(b) to (d), it is seen that the temperature-limited speed remained constant at about 99 percent of rated speed for all altitudes up to 50,000 feet. This unusual trend resulted from the compensating effects of decreasing ambient air temperature and reductions in compressor efficiency (ref. 1) as the altitude was increased. Net thrust exhibited the expected trend of first decreasing and then increasing as the true airspeed was increased from the static condition. Inasmuch as the fuel flow increased continuously with true airspeed, the specific fuel consumption also increased. For example, at rated sea-level static conditions the specific fuel consumption obtained from figure 10(a) was 0.956 pound of fuel per hour per pound of net thrust. At an airspeed of 650 knots, this value increased to 1.328.

The effects of increasing altitude on engine performance result from the following factors: (1) a reduction in ambient pressure, which reduces the engine air flow; (2) a reduction in ambient air temperature, which permits operation at higher corrected engine speeds with higher engine pressure and temperature ratios; (3) Reynolds number effects, which decrease the corrected air flow, the compressor efficiency, and sometimes the turbine efficiency; and (4) decreased combustion efficiency primarily due to reductions in combustor-inlet pressure. The first two effects can be predicted from sea-level data by use of the common correction factors δ and θ. Determination of the remaining altitude effects requires engine performance data at simulated altitude conditions. For example, if the performance of this engine were predicted at 95 percent of rated speed, an altitude of 50,000 feet, and an airspeed of 461 knots (Mach number of 0.8) on the basis of sea-level performance data, the net thrust would be about 1360 pounds compared with an actual value of 1367 pounds (see fig. 10(d)). The unusually close agreement of the predicted and actual thrusts for this engine is attributed to the increase in engine temperature ratio as the Reynolds number index was reduced; this increase balanced the detrimental effects of reduced Reynolds number on both engine air flow and compressor efficiency. The actual specific fuel consumption, however, was 1.161 pounds per hour per pound of net thrust, which is an increase of 3.4 percent over the predicted value of 1.122.

On the basis of the curves given in figures 6 to 9, the effects of nonstandard inlet-air temperature may also be calculated. For example, at take-off conditions and 99.4 percent of rated engine speed, the effect of increasing the ambient air temperature from 59° to 100° F would be to reduce the thrust by 9.4 percent and increase the specific fuel consumption 1.1 percent.

In-flight thrust determination. - In order to facilitate the determination of engine thrust in flight and also to avoid using equation (5) in appendix B to determine the thrust of this engine configuration, jet thrust is given in figure 11 as a function of the quantity $(1.26P_7 - p_0)$. The correlation of these quantities is derived in reference 4. It is seen that the experimental correlation is good. For the exhaust-nozzle area used (20.95-inch cold diameter), the jet thrust is about 2.4 times the quantity $(1.26P_7 - p_0)$. If the exhaust nozzle is trimmed to a slightly different diameter, the thrust values given by figure 11 must be adjusted by multiplying the value from figure 11 by the ratio of the area actually used to the area used in this investigation. The use of figure 11 is also illustrated in the sample calculation of appendix C. It should be noted that this method of in-flight thrust determination is not valid when an ejector-exit configuration is employed, because of the effect of the ejector on the static pressure at the exhaust-nozzle outlet.

In using this method of measuring thrust, it is important to obtain an accurate average value of total pressure in the exhaust nozzle because of the existence of large total-pressure gradients. Typical total-pressure profiles are shown in figure 12 for several operating conditions. In this figure each symbol represents the average value obtained at a given radius from rakes located 90° apart (see fig. 4(b)). Examination of profiles for a large number of test points shows that an average from four total-pressure probes located at 78 percent of the nozzle radius gives the over-all average total pressure within ±0.3 percent for this particular engine.

CONCLUDING REMARKS

From this investigation of the J73-GE-1A turbojet engine, sufficient data have been obtained and presented in the form of engine pumping characteristics to allow calculation of complete engine performance at all flight conditions with Reynolds number index values between 0.90 and 0.20 at corrected engine speeds above 6700 rpm. Although air flow data are not available, pumping-characteristic curves are also presented for Reynolds number index values of 0.16, 0.14, and 0.13 to aid in estimating the engine performance at extreme altitudes. Curves of net thrust and fuel flow, calculated from the pumping characteristics, are also given as functions of true airspeed for several altitudes.

For a given engine speed, the values of net thrust obtained with this engine at altitudes up to 50,000 feet agreed closely with the predicted values from sea-level data. However, the detrimental effects of increasing altitude on the over-all engine performance were evident in the higher specific fuel consumptions incurred at altitude compared with the values predicted from sea-level data. Specific fuel consumption also increased with increased flight Mach number or airspeed. The effect of having an ambient air temperature of 100° F instead of the standard 59° F at approximate take-off conditions was to reduce the net thrust of this engine by 9.4 percent and increase the specific fuel consumption by 1.1 percent.

Data are also presented to enable the determination of thrust in flight by measurements of total pressure at the exhaust-nozzle inlet and of ambient static pressure. Optimum immersion of the total-pressure probes and also possible errors due to the pressure profile are discussed briefly.

Lewis Flight Propulsion Laboratory
National Advisory Committee for Aeronautics
Cleveland, Ohio, October 6, 1953

APPENDIX A

SYMBOLS

The following symbols are used in this report:

A	cross-sectional area, sq ft
B	force exerted on test-bed, lb
C_D	exhaust-nozzle flow coefficient
F_j	jet thrust, lb
F_n	net thrust, lb
f	fuel-air ratio
g	acceleration due to gravity, 32.2 ft/sec^2
h	enthalpy, Btu/lb
M_0	flight Mach number
N	engine speed, rpm
P	total pressure, lb/sq ft abs
p	static pressure, lb/sq ft abs
R	gas constant, 53.4 ft-lb/(lb)($^{\circ}$R)
T	total temperature, $^{\circ}$R
t	static temperature, $^{\circ}$R
V	velocity, ft/sec
W_a	air flow, lb/sec
W_f	fuel flow, lb/hr
W_f/F_n	specific fuel consumption, lb/(hr)(lb net thrust)
γ	ratio of specific heats
δ	ratio of engine-inlet total pressure to absolute static pressure of NACA standard atmosphere at sea level

$\delta/\varphi\sqrt{\theta}$	Reynolds number index
η_b	combustion efficiency
θ	ratio of absolute total temperature at engine inlet to absolute static temperature of NACA standard atmosphere at sea level
λ	$\frac{A_m + B}{m + 1}$ (see ref. 3), Btu/lb fuel
ρ	density, slugs/cu ft
φ	ratio of absolute viscosity of air at engine inlet to absolute viscosity of NACA standard atmosphere at sea level

Subscripts:

a	air
i	indicated
R	rated
r	rake
s	scale
t	exhaust-nozzle throat
x	engine-inlet duct
0	altitude test chamber
1	engine inlet
6	turbine outlet
7	exhaust-nozzle inlet

APPENDIX B

METHODS OF CALCULATION

Total temperatures were calculated from thermocouple-indicated temperatures with the equation

$$T = \frac{T_i\left(\frac{P}{p}\right)^{\frac{\gamma-1}{\gamma}}}{1 + \alpha\left[\left(\frac{P}{p}\right)^{\frac{\gamma-1}{\gamma}} - 1\right]} \tag{1}$$

An experimentally determined value of 0.85 was used for the thermocouple impact-recovery factor α.

Air flow. - Engine-inlet air flow was determined from pressure and temperature instrumentation at station 1 by use of the equation

$$W_{a,1} = g\rho_1 A_1 V_1 = A_1\sqrt{\frac{2g}{R}}\left(\frac{p_1}{\sqrt{T_1}}\right)\sqrt{\left(\frac{\gamma_1}{\gamma_1 - 1}\right)\left(\frac{P_1}{p_1}\right)^{\frac{\gamma_1-1}{\gamma_1}}\left[\left(\frac{P_1}{p_1}\right)^{\frac{\gamma_1-1}{\gamma_1}} - 1\right]} \tag{2}$$

The various compressor-outlet bleed flows and compressor-leakage air flow were determined to be about 2 percent of the engine-inlet air flow. All bleed and leakage flows rejoined the main-stream flow before reaching the exhaust nozzle.

Combustion efficiency. - Combustion efficiency is defined as the ratio of the actual enthalpy rise through the combustor to the theoretical maximum enthalpy rise. The following equation was used to calculate combustion efficiency:

$$\eta_b = \frac{h_{a,7} + f\lambda_7 - h_{a,1}}{18,700f} \tag{3}$$

Thrust coefficient. - The nozzle thrust coefficient, which was used to adjust rake thrust to actual thrust, was calculated as the ratio of the jet thrust obtained from force measurements on the test bed to the rake jet thrust. Thrust based on force measurements (scale thrust) was obtained from the equation

$$F_{j,s} = B + \frac{W_{a,1}V_x}{g} + A_x(p_x - p_0) \tag{4}$$

The ideal or rake jet thrust, based on the survey at the exhaust-nozzle inlet, was obtained from the following expression:

$$F_{j,r} = (1+f)W_{a,1}\sqrt{\frac{2R}{g}\,\frac{\gamma_7 T_7}{(\gamma_7 - 1)}\left[1 - \left(\frac{p_t}{P_7}\right)^{\frac{\gamma_7-1}{\gamma_7}}\right]} + C_D A_t(p_t - p_0) \tag{5}$$

When the jet velocity is subsonic, $\left[P_7/p_0 < \left(\frac{\gamma + 1}{2}\right)^{\frac{\gamma}{\gamma-1}}\right]$, and $p_t = p_0$, equation (5) becomes

$$F_{j,r} = (1+f)W_{a,1}\sqrt{\frac{2R}{g}\,\frac{\gamma_7 T_7}{(\gamma_7 - 1)}\left[1 - \left(\frac{p_0}{P_7}\right)^{\frac{\gamma_7-1}{\gamma_7}}\right]} \tag{6}$$

Net thrust was obtained by subtracting the equivalent momentum of the air at the engine inlet from the jet thrust

$$F_{n,s} = F_{j,s} - \frac{W_{a,1}V_0}{g} \tag{7}$$

where V_0 is given by the equation

$$V_0 = \sqrt{\frac{2\gamma_1 gRT_1}{\gamma_1 - 1}\left[1 - \left(\frac{p_0}{P_1}\right)^{\frac{\gamma_1-1}{\gamma_1}}\right]} \tag{8}$$

with complete ram-pressure recovery assumed.

The ratio of hot exhaust-nozzle area to cold exhaust-nozzle area was taken as 1.01 for all calculations herein.

APPENDIX C

SAMPLE CALCULATIONS

In order to illustrate the use of the engine pumping characteristics, a problem is assumed at random as follows:

It is desired to determine the net thrust and specific fuel consumption of a J73-GE-1A engine operating in an airplane at the following conditions:

Pressure altitude, ft	38,000
Ambient pressure, p_0, lb/sq ft	431
Flight Mach number, M_0	0.80
Ambient air temperature, $^{\circ}F$	0
Engine speed, N, rpm	7800
Ram-pressure recovery	0.95

It is assumed that for the airplane in question a nonstandard tail pipe is required such that 0.04 of the total pressure is lost between the turbine outlet and the exhaust nozzle.

Engine-inlet conditions are calculated as follows:

$$p_0 \text{ (given)} = 431 \text{ lb/sq ft}$$

$$T_1 = t_0\left(1 + \frac{\gamma-1}{2} M_0^2\right) = 460\left[1 + 0.2(0.8)^2\right] = 519^{\circ} \text{ R}$$

$$\theta = T_1/519 = 1.00$$

$$N/\sqrt{\theta} = 7800 \text{ rpm}$$

$$P_1 = p_0 + 0.95p_0\left[(1 + 0.2M_0^2)^{3.5} - 1\right] = 645.8 \text{ lb/sq ft}$$

$$\varphi = 1.00, \text{ since } \theta = 1.0$$

$$\delta = 645.8/2116 = 0.305$$

$$\delta/\varphi\sqrt{\theta} = \delta = 0.305$$

$$\frac{N/\sqrt{\theta}}{(N)_R} = \frac{7800}{7950} = 0.981$$

From these values, the engine temperature ratio and pressure ratio may be determined as follows:

At 98.1 percent of rated corrected engine speed and at a Reynolds number index of 0.305, the engine total-pressure ratio and engine total-temperature ratio are given in figure 6 as approximately 2.15 and 3.21, respectively. The exhaust-gas temperature is then

$$T_7 = 3.21T_1 = 1666^{\circ}\ R$$

and the total pressure for the standard engine at the exhaust nozzle would be

$$P_7 = 2.15P_1 = 1388\ \text{lb/sq ft}$$

In order to allow calculations for engines with nonstandard tail-pipe installations, the tail-pipe pressure losses for the standard tail pipe are presented in figure 13 as a basis for a correction factor. For the engine in question, the exhaust-nozzle total pressure is then

$$P_7 = 1388\ \frac{1 - 0.040}{1 - 0.028} = 1371\ \text{lb/sq ft abs}$$

where 0.028 is the value of $(P_6 - P_7)/P_6$ for the standard engine and 0.040 is the value for the engine in question.

From figure 7, the corrected air flow at a corrected speed of 7800 rpm is

$$\frac{W_a\sqrt{\theta}}{\delta} = 137.4\ \text{lb/sec}$$

and, since θ equals unity,

$$W_a = 137.4\ \frac{645.8}{2116} = 41.9\ \text{lb/sec}$$

The temperature rise across the engine $(T_7 - T_1)$ is $(1666^{\circ} - 519^{\circ})$ or 1147° R. From figure 9, the ideal fuel-air ratio is 0.0161. The combustion parameter W_aT_7 is (41.9×1666) or 6.98×10^4. Hence, from figure 8, the actual combustion efficiency is 0.96. The actual fuel-air ratio is then (0.0161/0.96) or 0.0168. The engine fuel flow is then given by the product of the air flow and the fuel-air ratio

$$W_f = W_a(f) = 41.9(0.0168) = 0.704 \text{ lb/sec}$$

or

$$W_f = 2535 \text{ lb/hr}$$

The jet thrust of the engine may be determined rapidly by the use of figure 11. The value of $(1.26P_7 - p_0)$ is 1296 pounds per square foot, and hence the jet thrust is given in figure 11 as 3090 pounds.

Jet thrust may be determined with more precision by the use of equation (5). At a temperature of 1666° R and a fuel-air ratio of 0.0168, γ_7 is 1.330. The value of the static pressure p_t at the throat of the exhaust nozzle may be determined from the following expression for critical pressure ratio:

$$\frac{P_7}{p_t} = \left(\frac{\gamma_7 + 1}{2}\right)^{\frac{\gamma_7}{\gamma_7 - 1}} = 1.850$$

Hence, p_t is 741 pounds per square foot. Substitution of these quantities into equation (5) results in a jet-thrust value of 3135 pounds. The thrust coefficient is 1.00; hence no correction is required. Net thrust is obtained by subtracting the momentum of the inlet air. Therefore,

$$F_n = F_j - W_a V_0/g = 2039 \text{ lb}$$

since

$$V_0 \doteq M_0\sqrt{\gamma g R T_0} = 842 \text{ ft/sec}$$

and

$$W_a V_0/g = (41.9)(842)/32.2 = 1096 \text{ lb}$$

The specific fuel consumption is 2535/2039 = 1.24 pounds of fuel per hour per pound of net thrust.

REFERENCES

1. Campbell, Carl E., and Sobolewski, Adam E.: Altitude-Chamber Investigation of J73-GE-1A Turbojet Engine Component Performance. NACA RM E53I08.

2. McAulay, John E., and Kaufman, Harold R.: Altitude Wind Tunnel Investigation of the Prototype J40-WE-8 Turbojet Engine Without Afterburner. NACA RM E52K10, 1953.

3. Turner, L. Richard, and Bogart, Donald: Constant-Pressure Combustion Charts Including Effects of Diluent Addition. NACA Rep. 937, 1949. (Supersedes NACA TN's 1655 and 1086.)

4. Hesse, W. J.: A Simple Gross Thrust Meter Installation Suitable for Indicating Turbojet Engine Gross Thrust in Flight. Tech. Rep. No. 2-52, Test Pilot Training Div., Naval Air Test Center, Apr. 3, 1952.

TABLE I. - ENGINE PERFORMANCE DATA FOR J73-GE-1A TURBOJET ENGINE

Run	Altitude, ft	Reynolds number index, $\frac{\delta_1}{\varphi_1\sqrt{\theta_1}}$	Ram-pressure ratio, P_1/p_0	Flight Mach number, M_0	Tank static pressure, p_0, $\frac{lb}{sq\ ft\ abs}$	Engine speed, N, rpm	Fuel flow, W_f, lb/hr	Engine-inlet-duct static pressure, p_x, $\frac{lb}{sq\ ft\ abs}$	Engine-inlet total pressure, P_1, $\frac{lb}{sq\ ft\ abs}$	Engine-inlet total temperature, T_1, °R	Turbine-outlet total pressure, P_6, $\frac{lb}{sq\ ft\ abs}$	Exhaust-nozzle-inlet total pressure, P_7, $\frac{lb}{sq\ ft\ abs}$	Exhaust-gas total temperature, T_7, °R	Engine total-pressure ratio, P_7/P_1	Engine total-temperature ratio, T_7/T_1
1	15,000	0.895	1.528	0.803	1185	7841	7500	1707	1811	499	4191	4087	1644	2.257	3.335
2		.893	1.511	.792	1194	7737	7120	1703	1804	499	4113	4003	1614	2.219	3.234
3		.899	1.520	.798	1191	7614	6680	1711	1810	498	3996	3885	1564	2.146	3.141
4		.898	1.513	.793	1193	7216	5380	1717	1805	498	3582	3484	1411	1.930	2.833
5		.910	1.533	.806	1192	6581	3370	1760	1827	498	2840	2787	1176	1.525	2.361
6	15,000	0.749	1.269	0.594	1193	7822	6160	1429	1514	499	3509	3396	1650	2.243	3.307
7		.749	1.277	.602	1179	7778	6125	1421	1506	497	3490	3393	1628	2.253	3.276
8		.761	1.284	.609	1184	7616	5670	1437	1520	495	3364	3272	1570	2.153	3.172
9		.750	1.279	.604	1181	7222	4530	1438	1511	497	2999	2916	1422	1.930	2.861
10		.759	1.272	.597	1191	6680	3120	1456	1515	496	2473	2426	1220	1.601	2.460
11	15,000	0.651	1.102	0.376	1197	7828	5450	1247	1319	499	3048	2966	1659	2.249	3.325
12		.661	1.112	.392	1187	7212	3955	1258	1320	495	2629	2557	1428	1.937	2.885
13		.668	1.118	.403	1187	6411	2345	1284	1327	493	2019	1980	1172	1.492	2.377
14	15,000	0.594	1.006	0.092	1183	7795	4855	1131	1190	494	2729	2657	1644	2.233	3.328
15		.588	.994	-----	1189	7598	4370	1126	1182	496	2609	2539	1578	2.148	3.181
16		.601	1.002	.055	1187	7222	3600	1139	1189	492	2391	2324	1440	1.955	2.927
17		.596	1.010	.118	1178	6407	2250	1155	1190	493	1886	1852	1221	1.556	2.477
18	25,000	0.590	1.526	0.802	781	7839	4900	1124	1192	495	2759	2682	1654	2.250	3.341
19		.593	1.524	.800	780	7786	4770	1121	1189	493	2735	2658	1633	2.235	3.312
20		.595	1.537	.809	778	7627	4235	1131	1196	494	2636	2561	1576	2.141	3.190
21		.589	1.529	.803	777	6551	2175	1144	1188	495	1843	1797	1176	1.513	2.376
22	35,000	0.550	1.912	1.009	486	7875	4480	872	929	435	2388	2336	1642	2.515	3.775
23		.551	1.898	1.003	490	7617	3930	874	930	436	2268	2217	1540	2.384	3.532
24		.541	1.912	1.009	489	7214	3240	883	935	440	2074	2018	1398	2.158	3.177
25		.531	1.912	1.009	491	6678	2300	897	939	449	1728	1688	1217	1.798	2.710
26	35,000	0.412	1.549	0.816	495	7848	3340	724	767	468	1827	1780	1665	2.321	3.558
27		.410	1.527	.802	490	7807	3290	704	748	461	1812	1775	1639	2.373	3.556
28		.377	1.538	.809	489	7797	3090	710	752	491	1732	1684	1661	2.239	3.383
29		.373	1.548	.816	487	7617	2800	714	754	497	1651	1601	1595	2.123	3.209
30		.408	1.538	.809	489	7616	3010	709	752	465	1739	1699	1569	2.259	3.374
31		.402	1.532	.806	491	7436	2770	711	752	471	1689	1641	1517	2.182	3.221
32		.401	1.548	.816	484	7214	2400	711	749	474	1555	1516	1434	2.024	3.025
33		.367	1.544	.813	493	7174	2205	726	761	504	1466	1422	1431	1.869	2.839
34		.388	1.546	.815	485	6676	1666	720	750	482	1273	1238	1242	1.651	2.577
35	49,000	0.247	1.787	0.950	254	7699	1930	431	454	468	1060	1045	1619	2.302	3.459
36		.242	1.754	.934	260	7623	1880	430	456	470	1051	1035	1594	2.270	3.391
37		.238	1.796	.955	251	7220	1500	428	449	475	925	910	1460	2.027	3.073
38		.250	1.761	.937	259	6964	1340	436	456	466	889	876	1364	1.921	2.927
39		.229	1.739	.926	257	6680	1050	439	447	486	756	742	1269	1.660	2.611
40	55,000	0.191	1.961	1.031	179	7661	1530	331	351	465	820	808	1630	2.302	3.505
41		.195	1.816	.965	197	7508	1441	349	356	461	807	794	1572	2.230	3.410
42		.195	1.940	1.022	183	7223	1270	345	355	464	751	741	1476	2.087	3.181
43		.193	1.873	.992	189	6958	1075	346	354	463	692	683	1381	1.929	2.983
44		.205	1.994	1.045	181	6674	892	342	361	464	633	624	1278	1.729	2.754

TABLE I. - Concluded. ENGINE PERFORMANCE DATA FOR J73-GE-1A TURBOJET ENGINE

Run	Air flow, W_a, lb/sec	Fuel-air ratio, f	Jet thrust, F_j, lb	Net thrust, F_n, lb	Specific fuel consumption, W_f/F_n, $\frac{lb}{(hr)(lb\ thrust)}$	Corrected engine speed, $N/\sqrt{\theta_1}$, rpm	Corrected air flow, $\frac{W_a\sqrt{\theta_1}}{\delta_1}$, lb/sec	Corrected fuel flow, $W_f/\delta_1\sqrt{\theta_1}$, lb/hr	Corrected fuel-air ratio, f/θ_1	Corrected jet thrust, F_j/δ_1, lb	Corrected net thrust, F_n/δ_1, lb	Corrected specific fuel consumption, $W_f/F_n\sqrt{\theta_1}$, $\frac{lb}{(hr)(lb\ thrust)}$	Corrected exhaust-gas temperature, T_7/θ_1, °R
1	124.3	0.0168	9530	6335	1.184	7996	142.3	8933	0.0175	11,170	7400	1.208	1731
2	123.0	.0161	9206	6085	1.170	7890	141.4	8517	.0167	10,799	7138	1.193	1679
3	121.7	.0153	8877	5769	1.158	7773	139.3	7972	.0159	10,377	6744	1.182	1630
4	114.7	.0130	7522	4609	1.167	7367	131.7	6437	.0135	8,816	5402	1.191	1470
5	101.7	.0092	5440	2817	1.196	6719	115.3	3984	.0096	6,300	3262	1.221	1225
6	103.8	0.0165	7475	5448	1.131	7977	142.4	8782	0.0172	10,450	7616	1.153	1716
7	103.3	.0165	7378	5340	1.147	7948	142.1	8793	.0172	10,366	7503	1.172	1700
8	102.8	.0153	7051	5003	1.133	7798	139.8	8082	.0160	9,815	6964	1.160	1647
9	96.0	.0131	5965	4065	1.114	7380	131.5	6481	.0137	8,351	5691	1.138	1485
10	86.9	.0100	4438	2738	1.140	6833	118.7	4459	.0105	6,200	3825	1.166	1276
11	90.2	0.0168	6156	5019	1.086	7983	141.9	8915	0.0175	9,874	8050	1.107	1725
12	84.0	.0131	4877	3777	1.047	7385	131.4	6492	.0137	7,818	6055	1.072	1498
13	70.5	.0092	3098	2176	1.078	6578	109.6	3838	.0097	4,941	3471	1.106	1234
14	81.5	0.0166	5243	4989	0.973	7990	141.3	8848	0.0174	9,322	8870	0.997	1728
15	79.0	.0154	4857	4857	.900	7772	138.3	8002	.0161	8,694	8694	.920	1651
16	75.3	.0133	4221	4082	.882	7417	130.5	6581	.0140	7,513	7266	.906	1519
17	63.4	.0099	2713	2460	.915	6574	109.8	4105	.0104	4,824	4374	.938	1286
18	81.5	0.0167	6198	4114	1.191	8027	141.2	8906	0.0175	11,001	7302	1.220	1735
19	81.2	.0163	6120	4051	1.177	7989	140.8	8712	.0172	10,894	7211	1.208	1720
20	80.1	.0147	5879	3817	1.110	7818	138.2	7679	.0154	10,400	6752	1.138	1656
21	65.9	.0092	3488	1799	1.209	6708	114.6	3966	.0097	6,212	3204	1.238	1234
22	70.0	0.0178	5769	3723	1.203	8602	146.1	11,147	0.0212	13,142	8481	1.314	1959
23	69.2	.0158	5402	3388	1.160	8311	144.2	9,755	.0188	12,290	7708	1.266	1833
24	66.6	.0135	4817	2860	1.133	7834	138.7	7,963	.0159	10,901	6472	1.230	1648
25	60.0	.0106	3817	2034	1.131	7180	125.8	5,571	.0123	8,600	4563	1.216	1407
26	54.0	0.0172	4274	2909	1.148	8265	141.5	9,704	0.0191	11,792	8026	1.209	1846
27	53.7	.0170	4157	2832	1.162	8283	143.1	9,875	.0191	11,760	8012	1.233	1846
28	50.9	.0169	3943	2634	1.173	8016	139.4	8,939	.0179	11,096	7412	1.205	1756
29	49.9	.0156	3721	2423	1.156	7784	136.9	8,029	.0163	10,441	6799	1.181	1665
30	53.2	.0157	4005	2675	1.125	8046	141.7	8,948	.0175	11,270	7527	1.188	1751
31	52.0	.0148	3785	2481	1.116	7806	139.5	8,183	.0163	10,651	6982	1.172	1672
32	49.6	.0134	3484	2223	1.079	7548	133.9	7,094	.0147	9,830	6280	1.130	1570
33	46.8	.0131	3066	1843	1.196	7280	128.1	6,223	.0135	8,527	5125	1.214	1474
34	44.1	.0105	2603	1473	1.131	6927	119.9	4,877	.0113	7,343	4155	1.174	1338
35	32.2	0.0167	2559	1632	1.183	8108	142.3	9,473	0.0185	11,927	7607	1.246	1795
36	31.8	.0164	2512	1609	1.168	8011	140.2	9,167	.0181	11,656	7466	1.227	1780
37	29.2	.0143	2139	1288	1.165	7547	131.6	7,389	.0156	10,081	6070	1.218	1596
38	29.3	.0127	2010	1179	1.137	7349	128.6	6,561	.0141	9,326	5471	1.200	1519
39	25.9	.0112	1554	809	1.298	6903	118.8	51137	.0120	7,357	3830	1.341	1355
40	25.4	0.0167	2024	1242	1.232	8093	145.0	9,745	0.0186	12,203	7488	1.302	1819
41	24.9	.0161	1875	1154	1.249	7966	139.4	9,088	.0181	11,145	6859	1.325	1770
42	23.9	.0148	1773	1044	1.216	7639	134.8	8,007	.0166	10,569	6223	1.286	1652
43	23.0	.0130	1568	844	1.216	7367	129.9	6,803	.0146	9,372	5284	1.287	1548
44	21.8	.0114	1453	777	1.148	7059	120.6	5,530	.0142	8,516	4554	1.352	1430

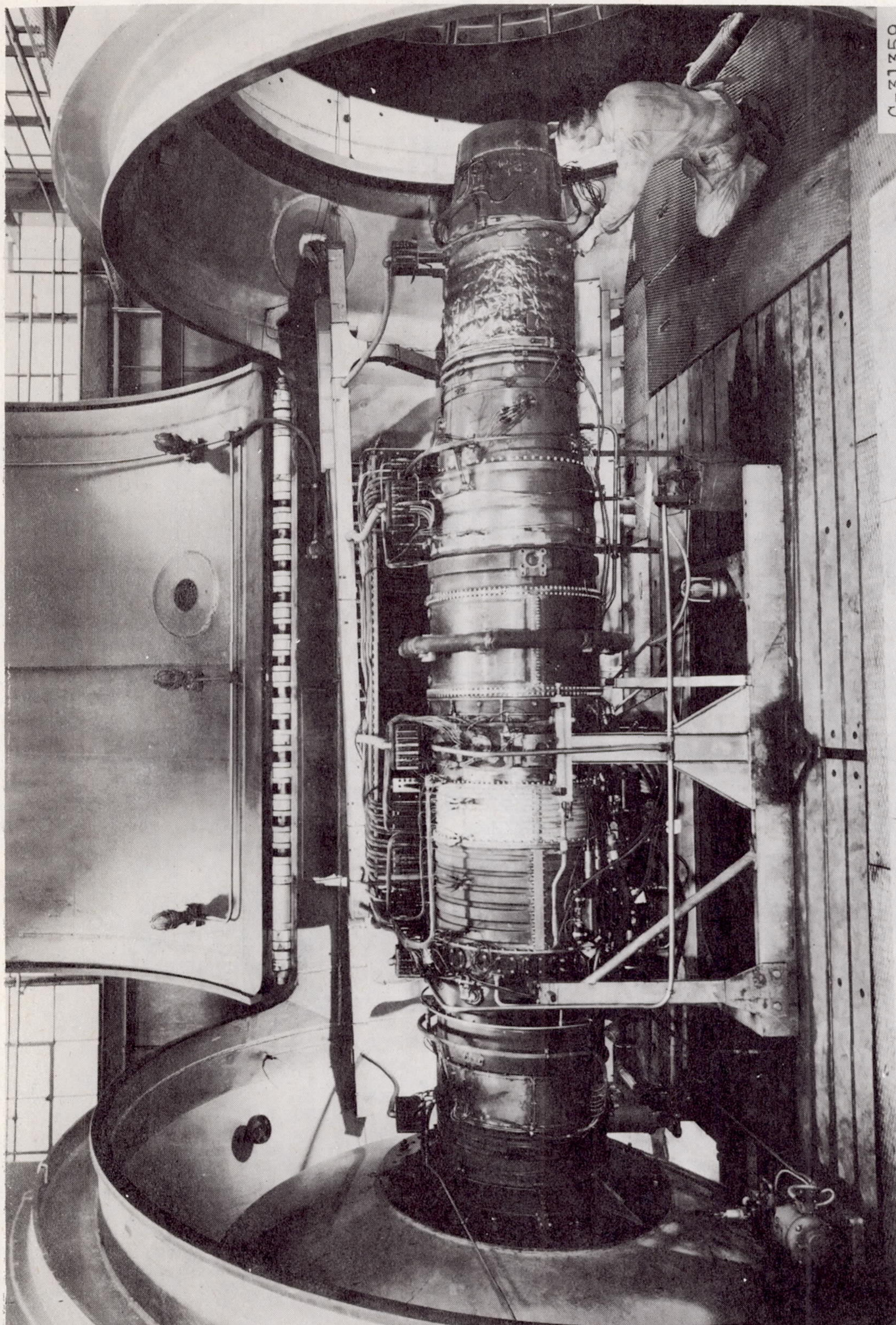

Figure 1. - View of J73-GE-1A engine in altitude chamber.

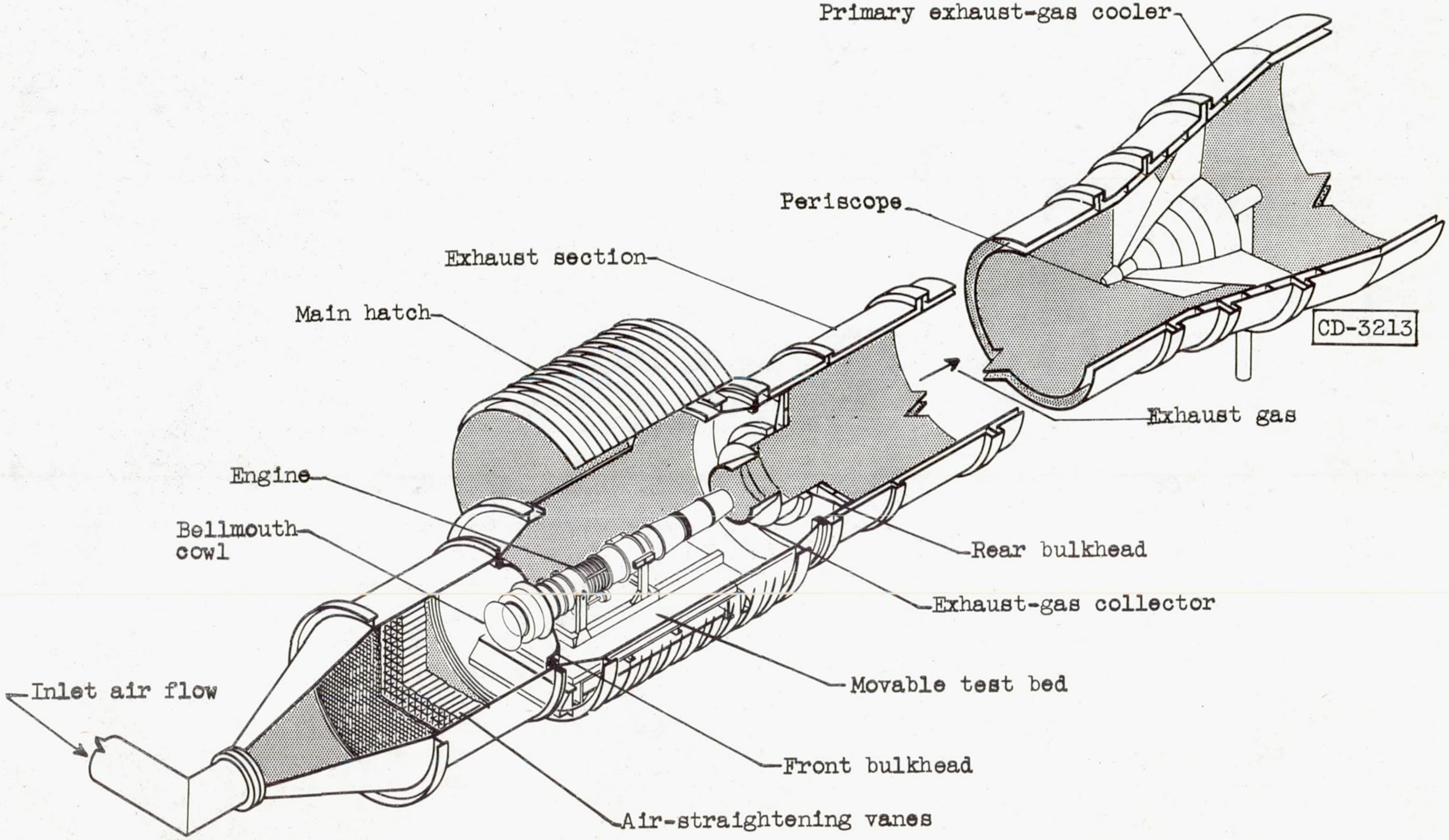

Figure 2. - Altitude chamber with engine installed in test section.

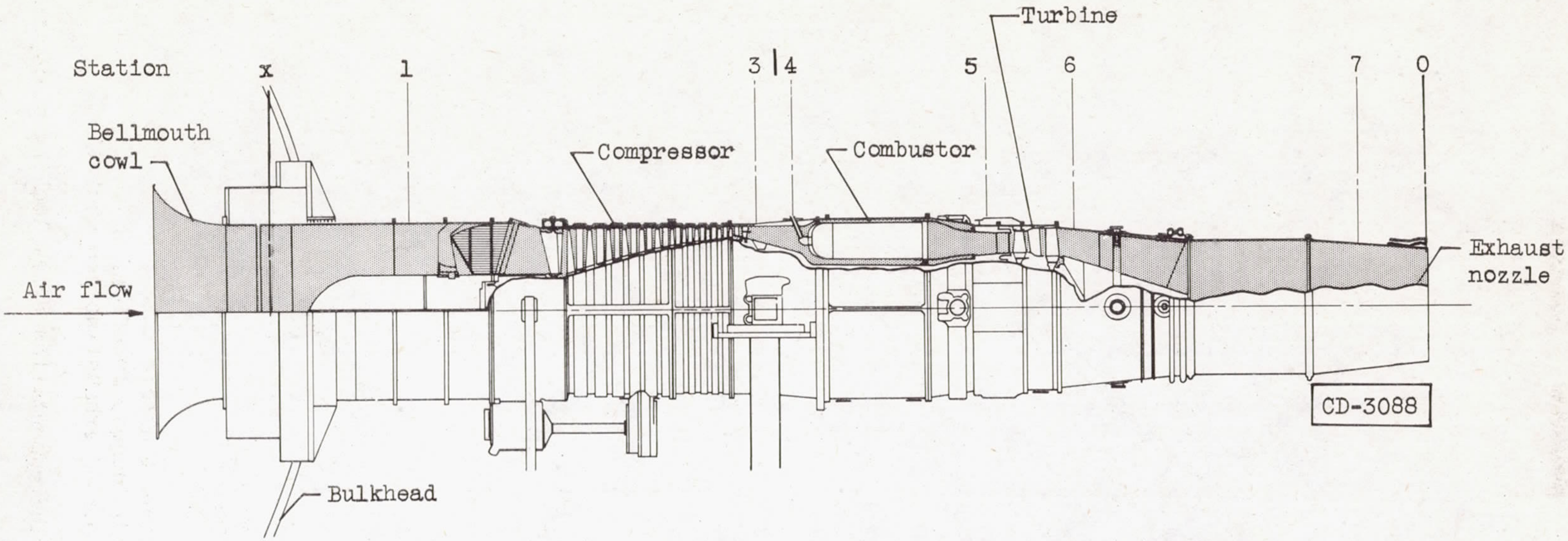

Station	Location	Total-pressure tubes	Static-pressure tubes	Wall static-pressure orifices	Thermo-couples
x	Engine-inlet duct	0	0	4	0
1	Engine inlet	36	16	4	16
3	Compressor outlet	20	4	5	6
4	Combustor inlet	10	0	0	0
5	Turbine inlet	9	0	0	0
6	Turbine outlet	24	0	8	20
7	Exhaust nozzle	28	16	4	20
0	Altitude test chamber	0	4	0	0

Figure 3. - Side view of turbojet engine showing instrumentation stations.

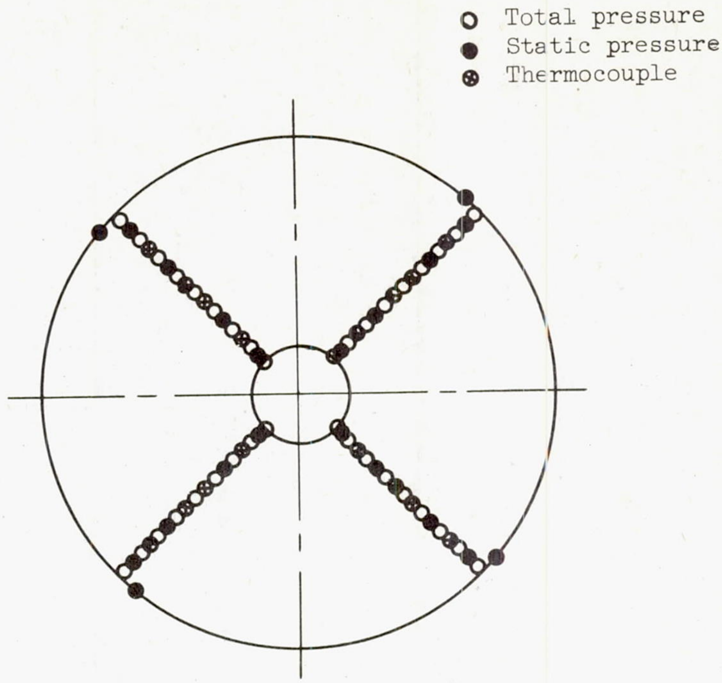

(a) Station 1, engine inlet. Passage height, 9.8 inches; location, 37 inches upstream of inlet guide vanes.

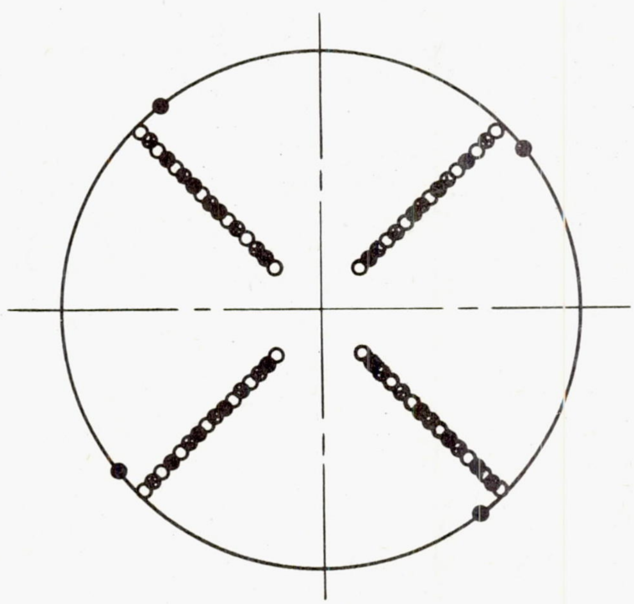

(b) Station 7, exhaust-nozzle inlet. Diameter, 23.5 inches; location, 11.8 inches upstream of exhaust-nozzle outlet.

Figure 4. - Location of instrumentation (view looking downstream).

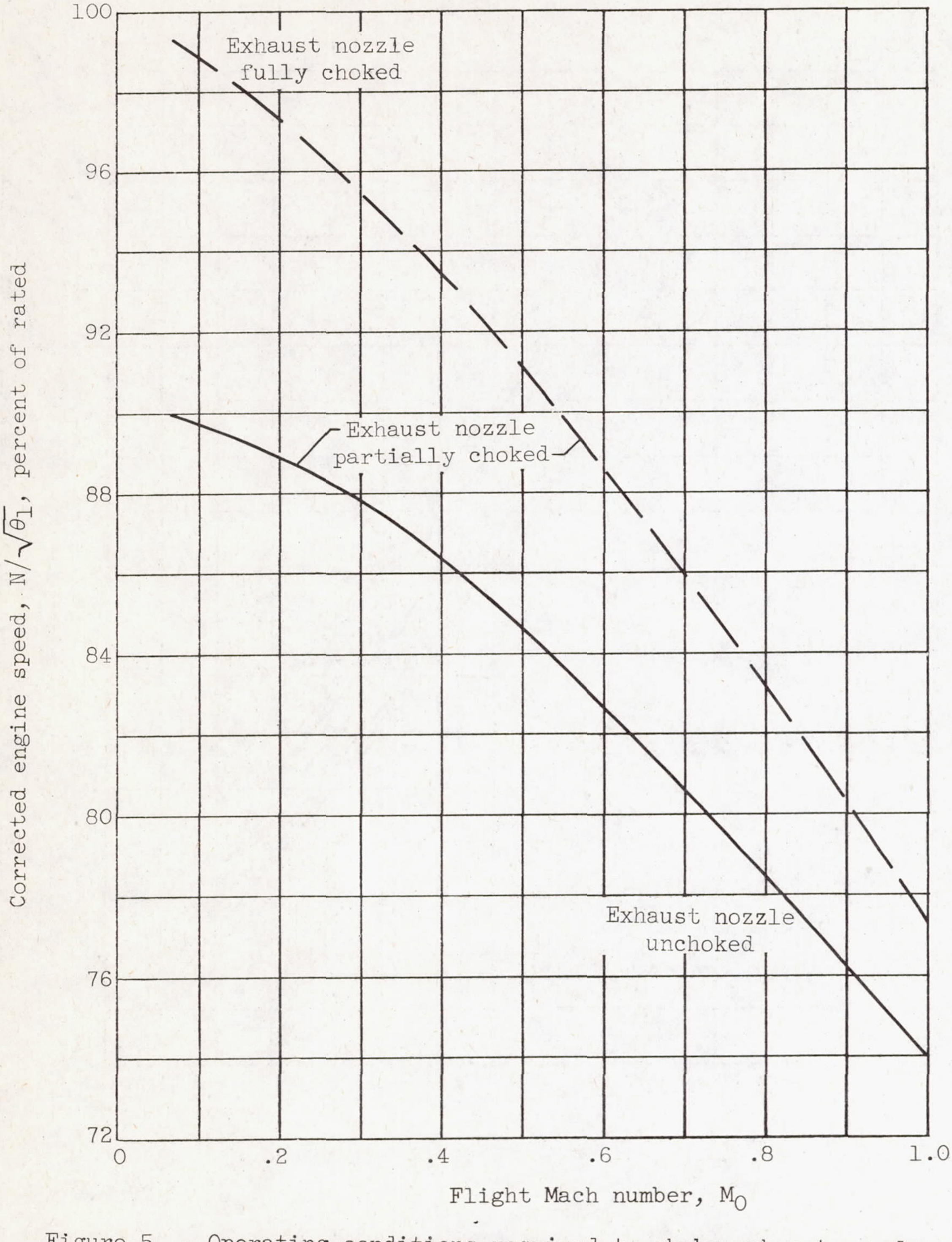

Figure 5. - Operating conditions required to choke exhaust nozzle.

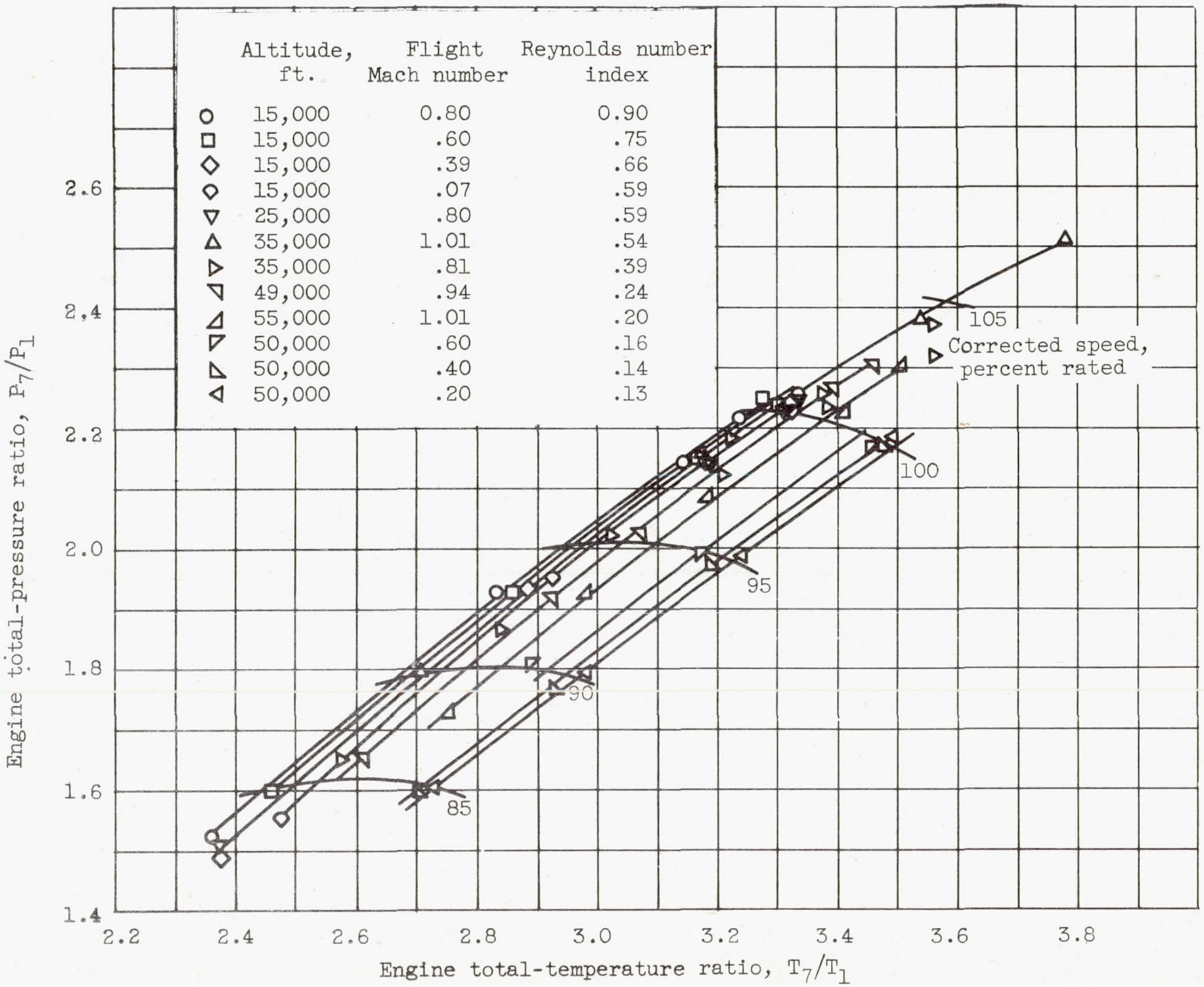

Figure 6. - Engine pumping characteristics. Exhaust-nozzle area, 345 square inches.

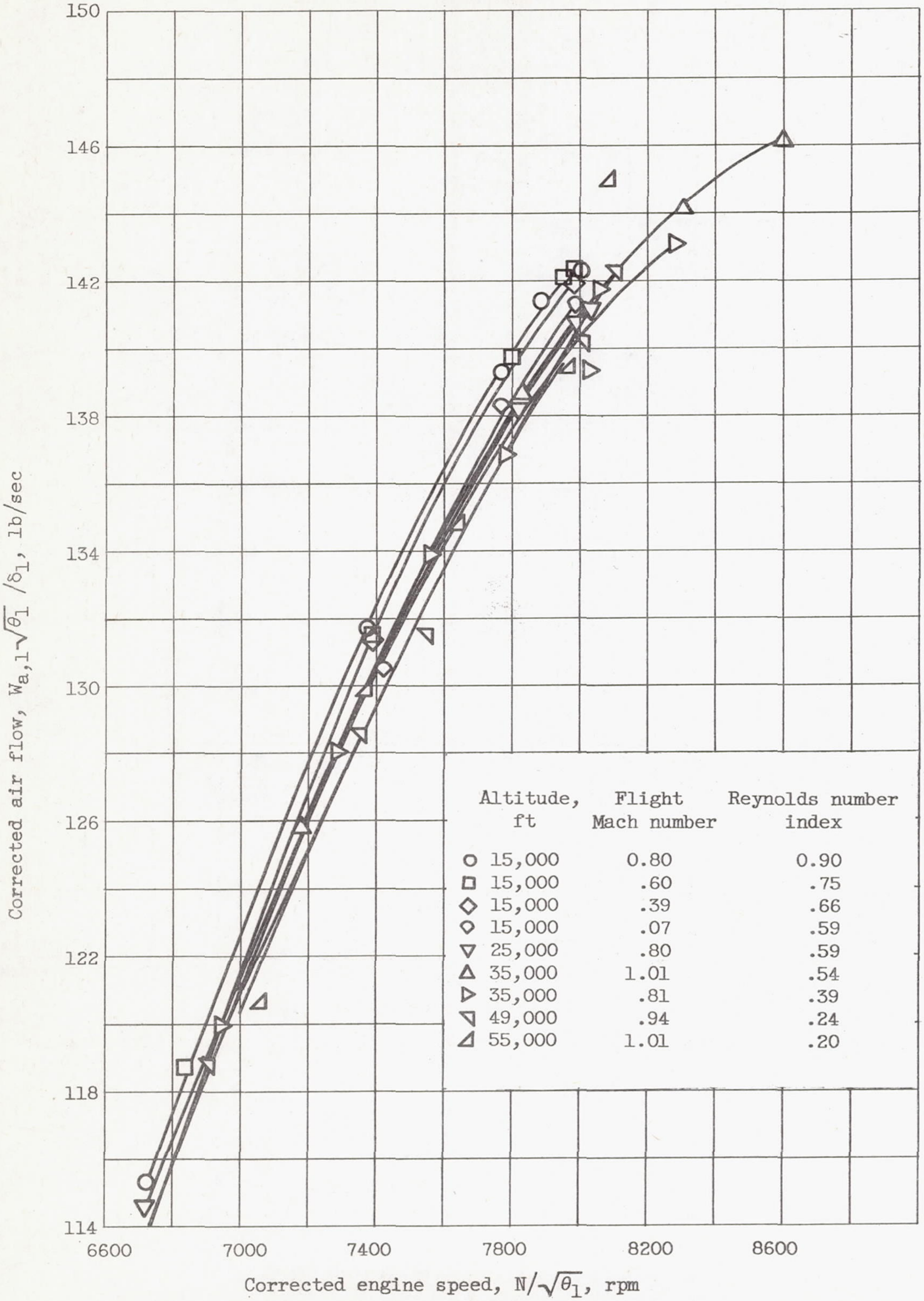

Figure 7. - Effect of Reynolds number index on engine air flow.

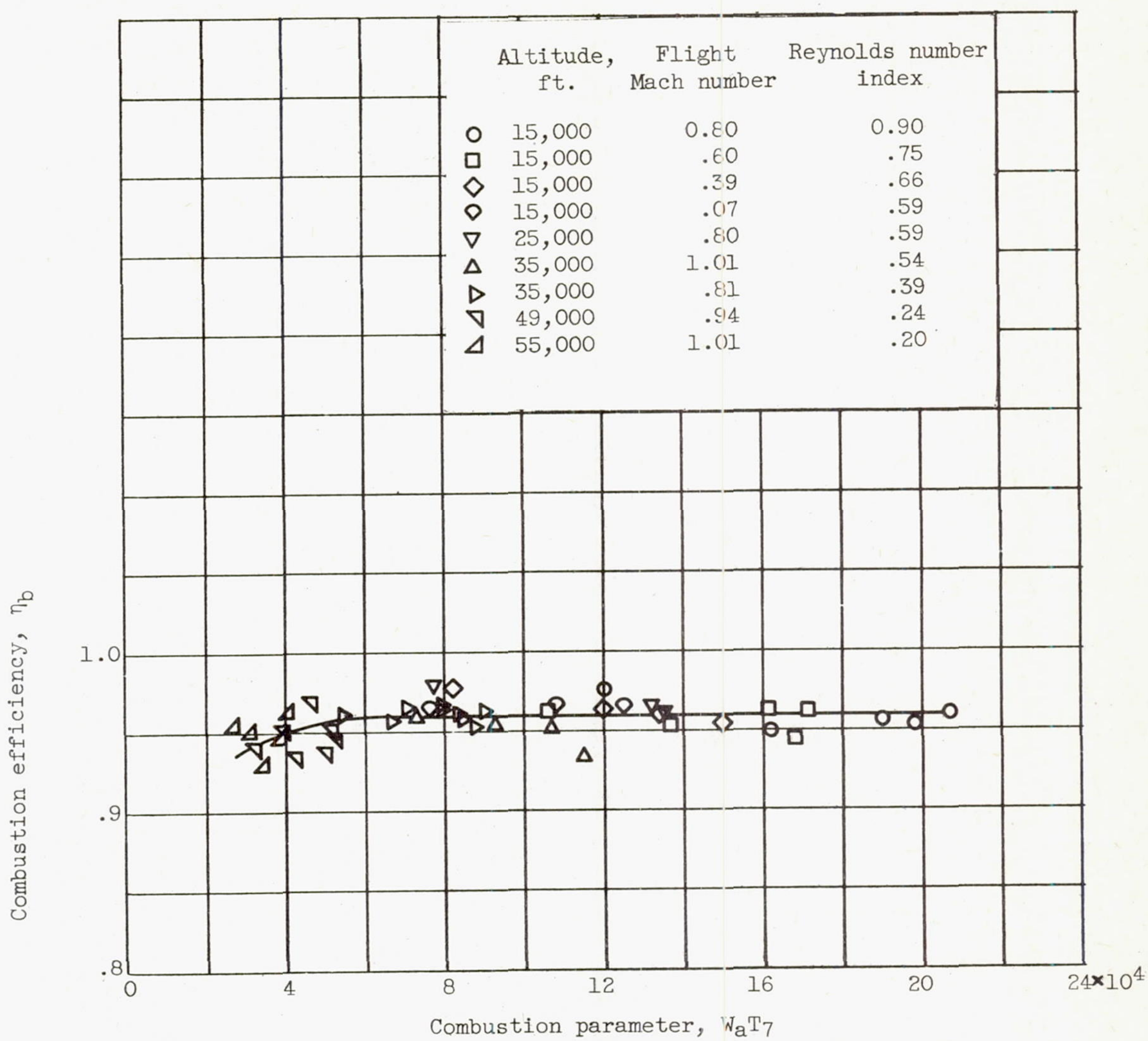

Figure 8. - Variation of engine combustion efficiency with combustion parameter.

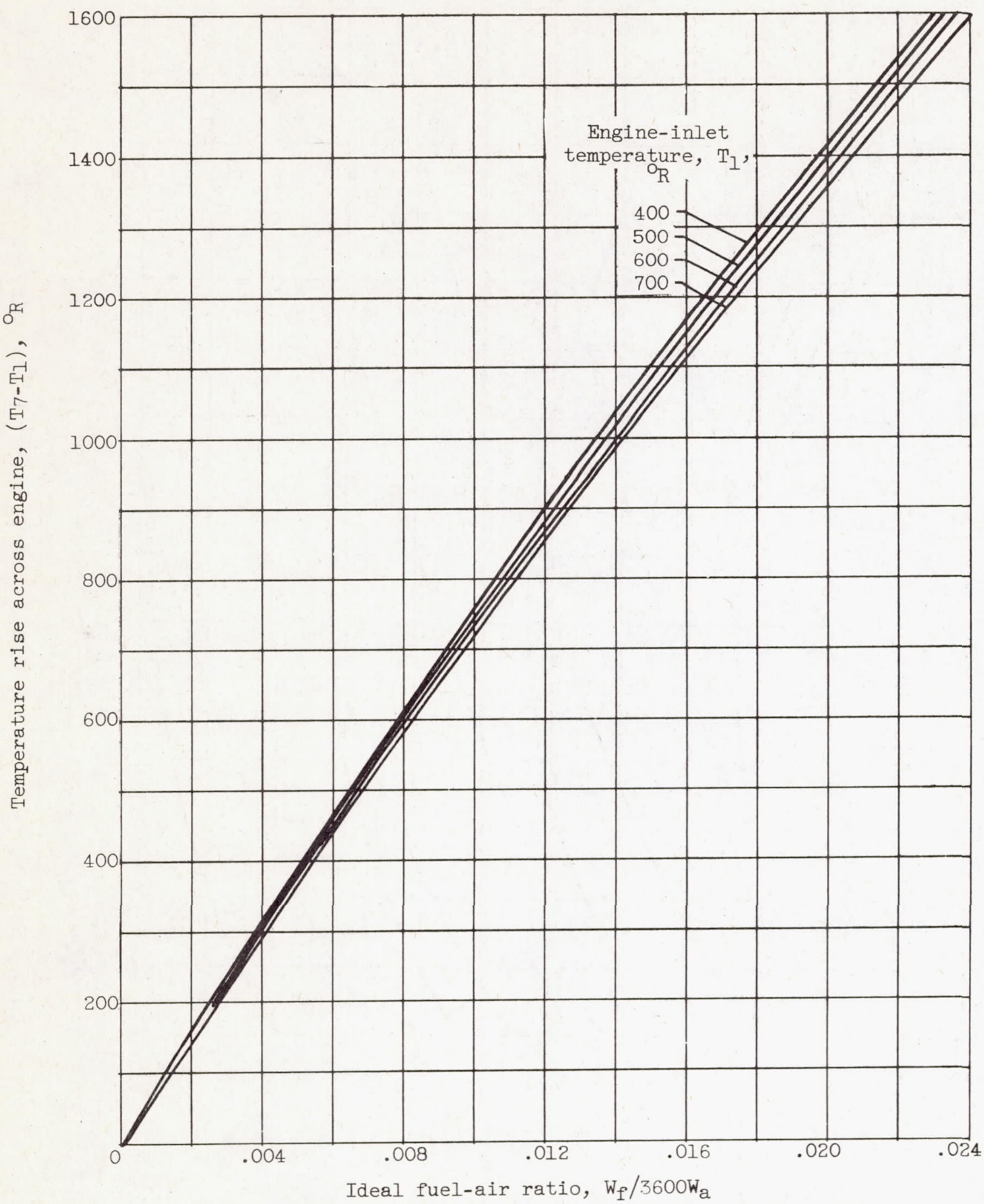

Figure 9. - Engine temperature rise as function of ideal fuel-air ratio. Lower heating value, 18,700 Btu per pound; hydrogen-carbon ratio, 0.171. (Data obtained from ref. 3).

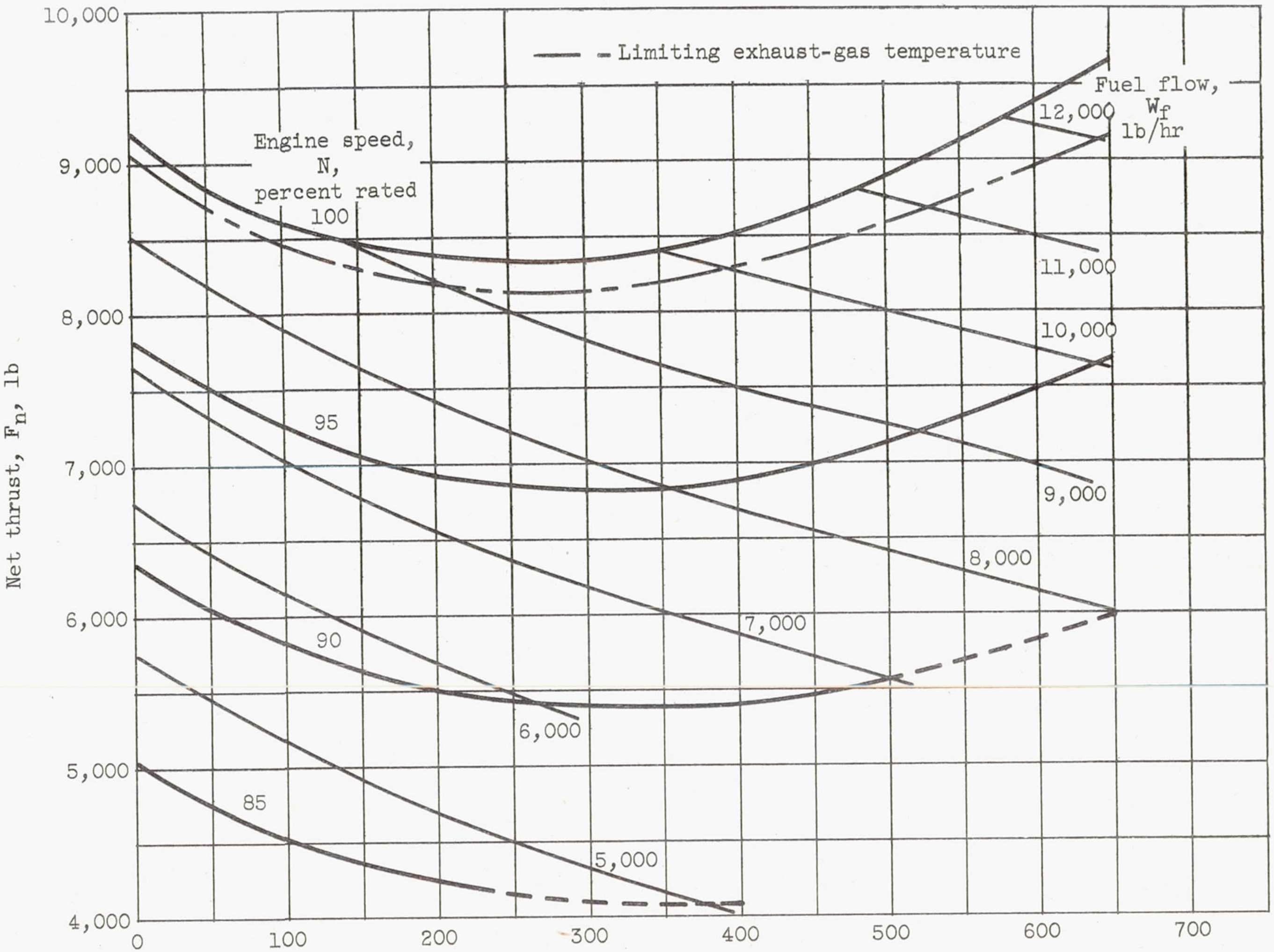

(a) Altitude, sea level.

Figure 10. - Variation of net thrust and fuel flow with true airspeed.

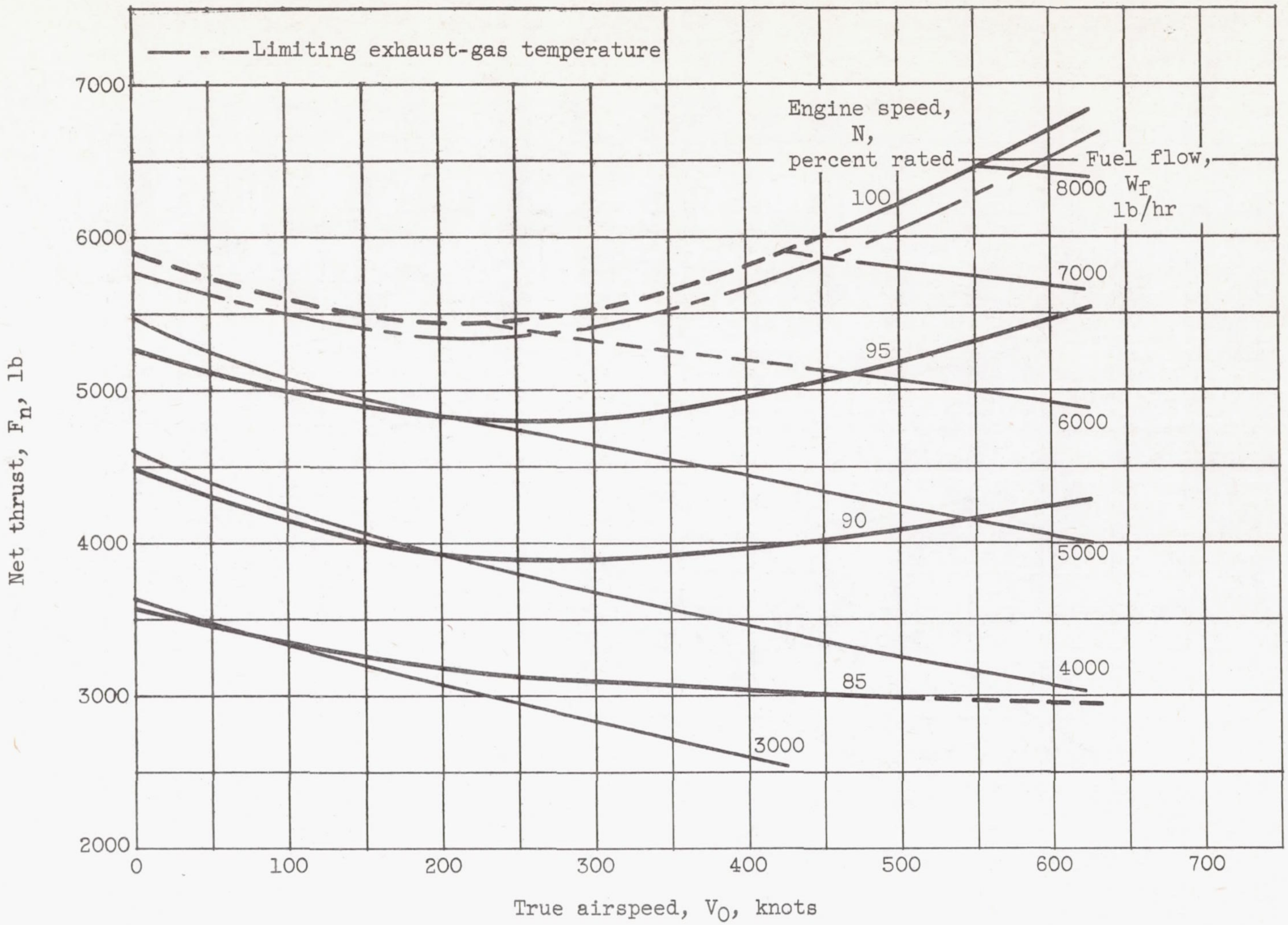

(b) Altitude, 15,000 feet.

Figure 10. - Continued. Variation of net thrust and fuel flow with true airspeed.

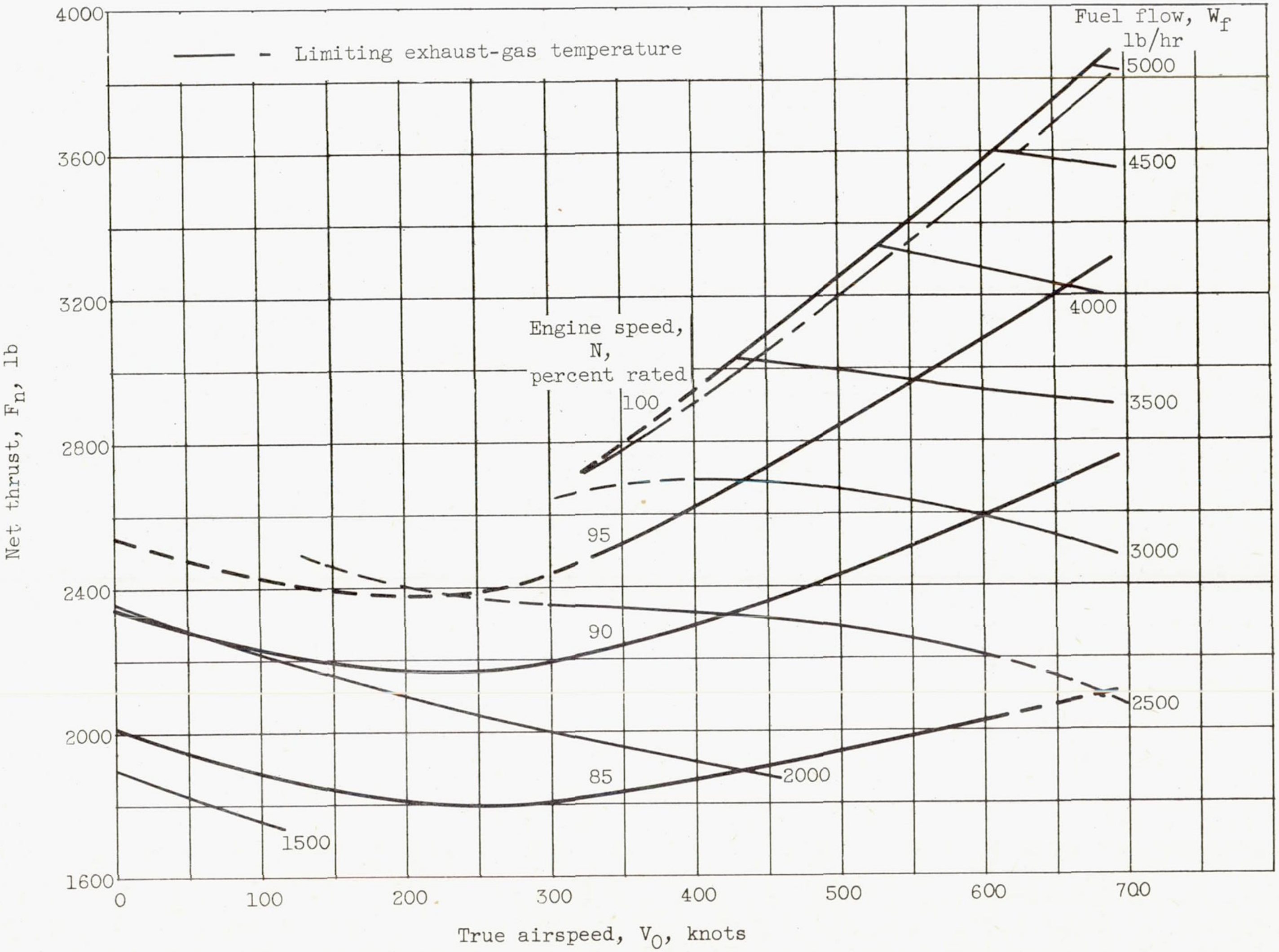

(c) Altitude, 35,000 feet.

Figure 10. - Continued. Variation of net thrust and fuel flow with true airspeed.

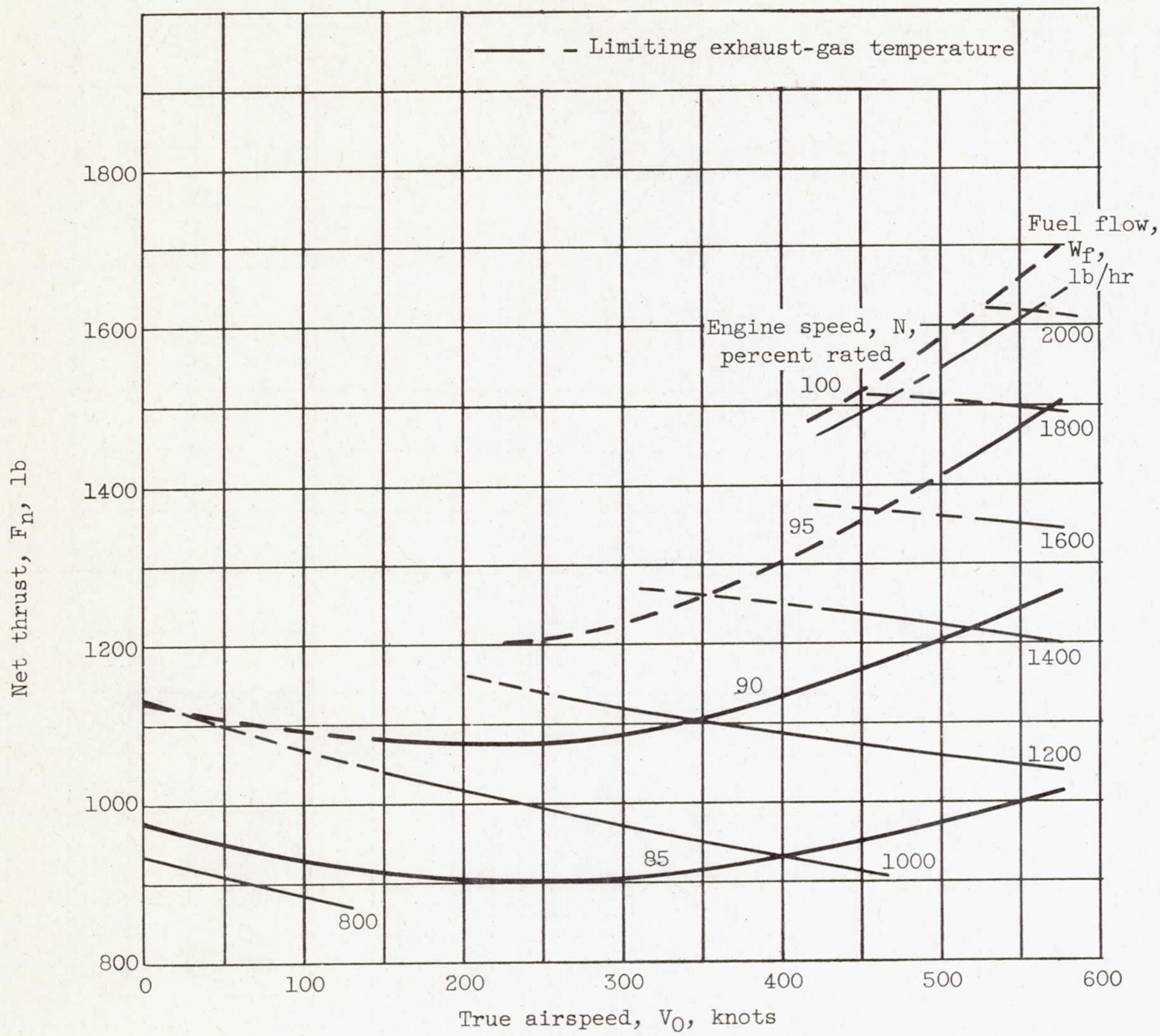

(d) Altitude, 50,000 feet.

Figure 10. - Concluded. Variation of net thrust and fuel flow with true airspeed.

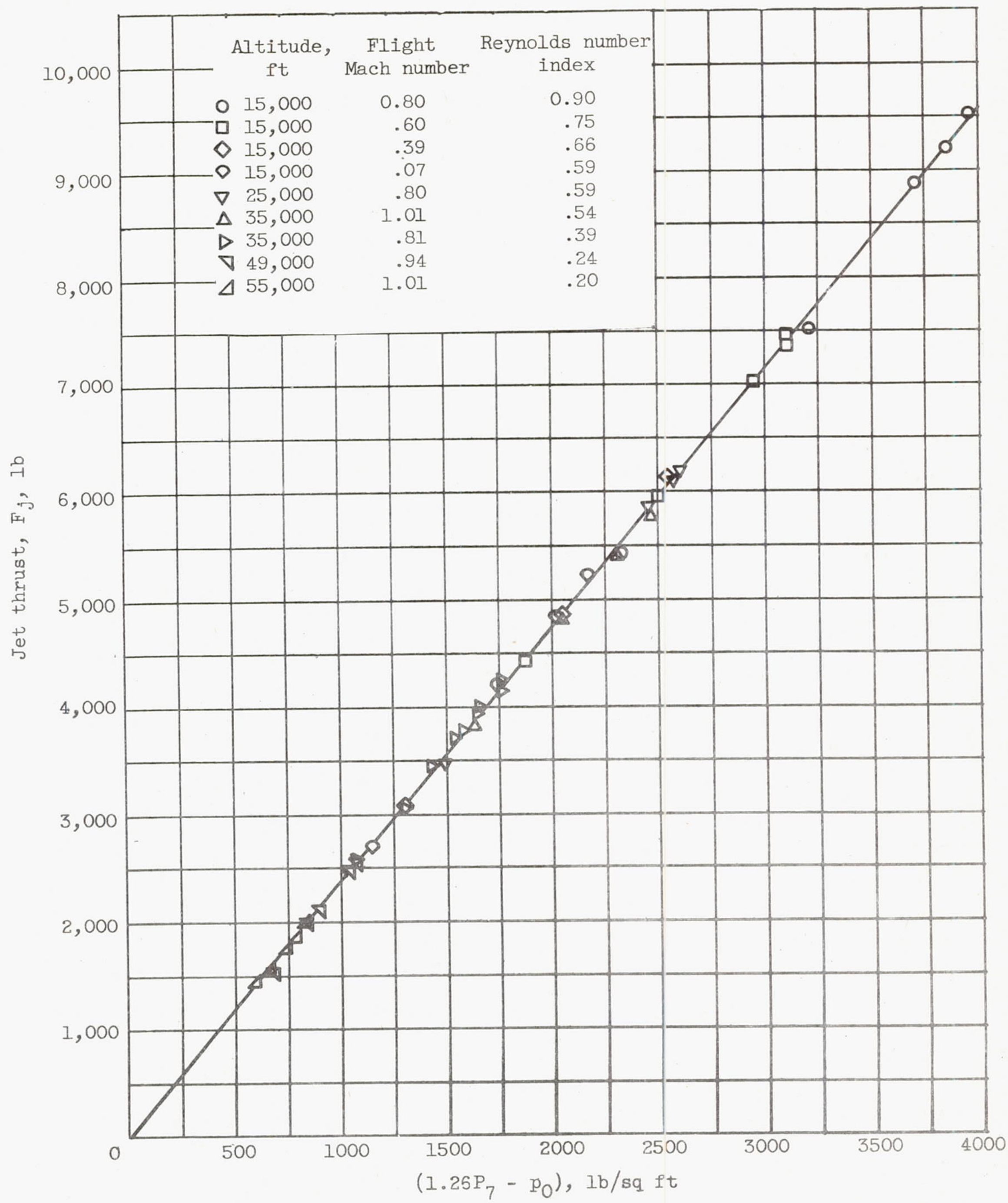

Figure 11. - Correlation of jet thrust with exhaust-nozzle total pressure and ambient static pressure.

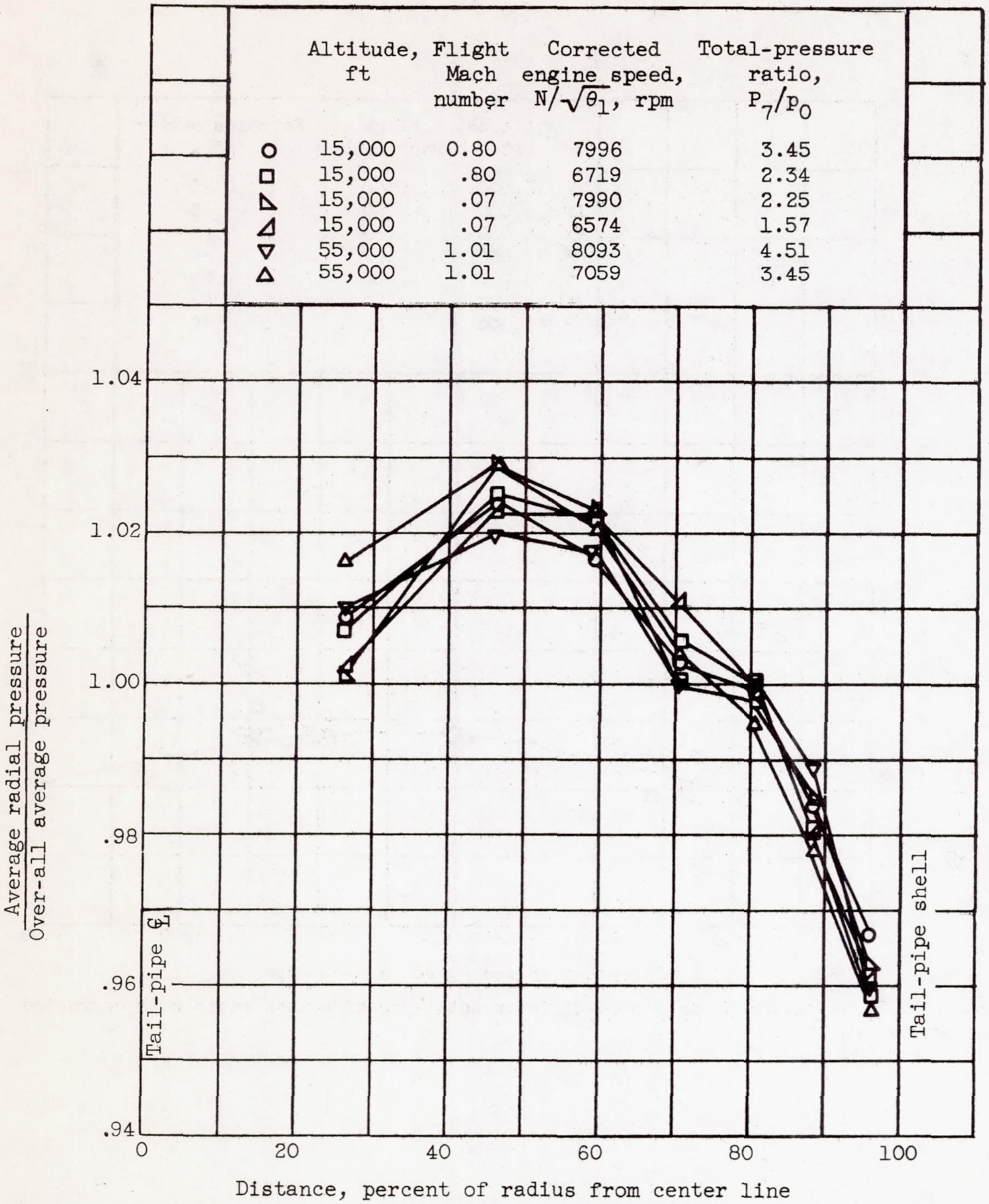

Figure 12. - Total-pressure profiles at exhaust-nozzle inlet, station 7 (4 rakes).

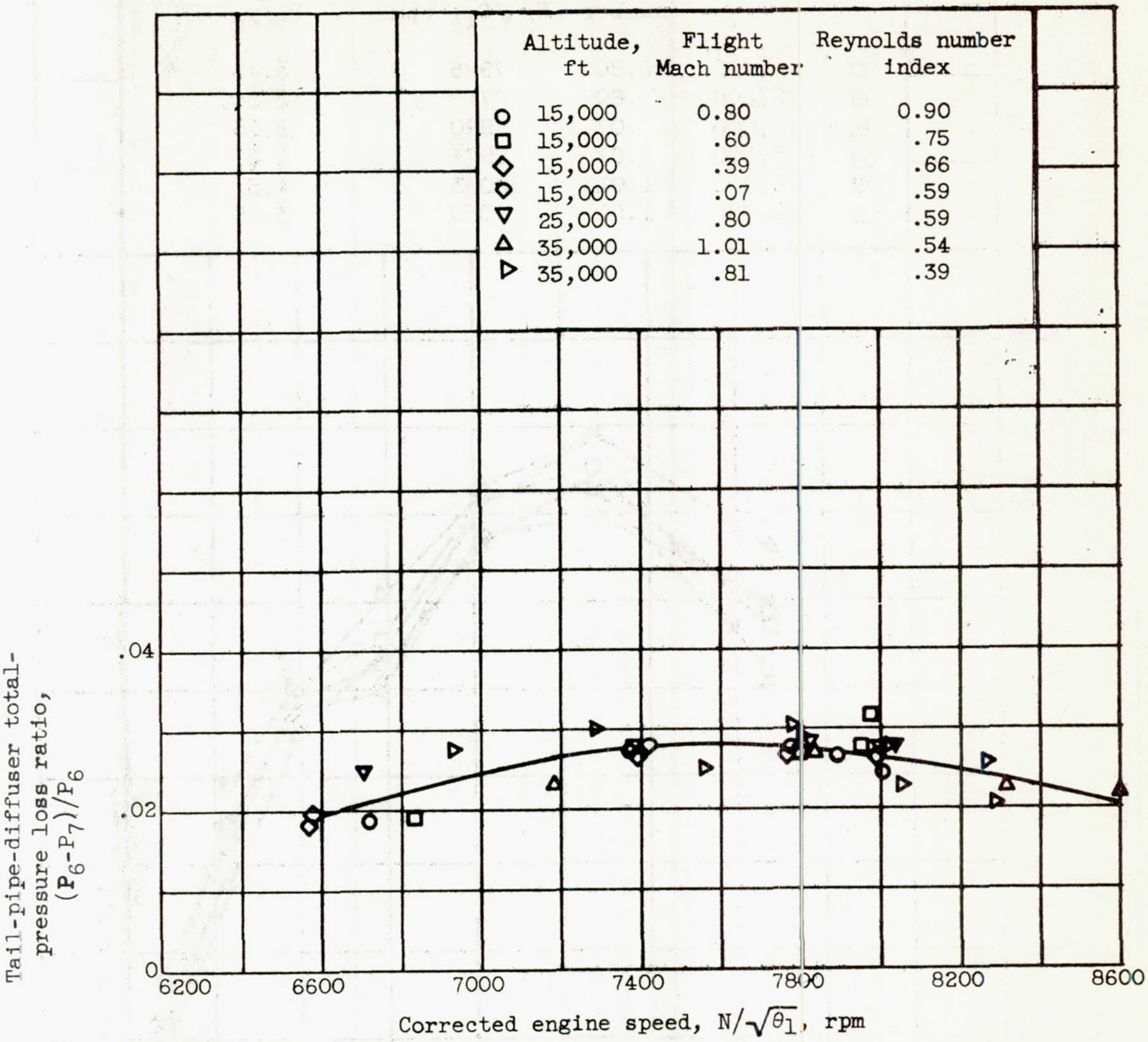

Figure 13. - Variation of tail-pipe-diffuser total-pressure loss ratio with corrected engine speed.